Pulsed electrodeposition of $CuInSe_2$ films for photovoltaic applications

Anna Palacios Padrós

Master's Thesis supervisors: Felipe Caballero-Briones[1,2], Fausto Sanz[3,2,4]

[1]CICATA-IPN Unidad Altamira. Km 14.5 Carretera Tampico-Puerto Industrial Altamira, 89600 Altamira, México. [2]Department of Physical Chemistry, Universitat de Barcelona, Martí i Franquès 1, 08028 Barcelona, Spain. [3]Institute for Bioengineering of Catalonia, Edifici Hèlix, Baldiri i Reixac 15-21, 08028 Barcelona, Spain. [4]CIBER-BBN, Campus Río Ebro, Edificio I+D Bloque 5, 1ª planta, Poeta Mariano Esquillor s/n, 50018 Zaragoza, Spain.

***Abstract*—Copper indium diselenide thin films have been prepared onto ITO (In_2O_3:Sn) substrates by a newly developed pulsed electrodeposition method. The proposed scheme consists of a cyclically repeated pulsed potential sequence at the corresponding deposition potentials of elemental Cu, Se and In. When the potential is stepped back to the initial Cu electrodeposition potential after a full cycle to start the subsequent three steps the excess of metallic In is dissolved and the formation of the desired CIS phase is enhanced. Two electrolyte concentrations and three different pulse durations were considered. The resulting films were compared to those grown with a program of potential sweep and step application. As grown films are nanocrystalline (112) oriented and p-type semiconducting with a bandgap around 1.1 eV. A second optical transition around 2.7-3.1 eV attributed to secondary Cu-Se phases was observed. Raman and photocurrent spectroscopies show a strong effect of the electrolyte concentration and pulse duration in the content of Se and Cu-Se unwanted phases, especially in the samples prepared at low concentration where Cu-Se is absent. The developed method represents a noticeable improvement in the phase purity and drops a hint towards the suppression of post-deposition treatments.**

***Index Terms*—6. Nanoenergy: $CuInSe_2$, electrodeposition, Raman spectroscopy, solar cells.**

I. Introduction

World annual energy consumption is predicted to grow from the current 13 terawattyears (TWyr) to 30 TWyr by 2050 [1]. Apart from facing the augment in demand, the global energy sector has to deal with the scarceness of fossil fuels and the climate change caused by the greenhouse gas emissions. Considering this, renewable sources have been proposed as the major candidates to tackle this future energy needs and among them photovoltaic energy is believed to be the only one with enough capacity to fulfil these challenges as 125000 TW of solar power strike the earth at any time [1].

Nowadays silicon is the material most widely used for the photovoltaic devices but the shortage of feedstock and the high manufacturing costs are restricting the expansion of the market [2]. New approaches like second generation solar cells based on heterojunction thin film technologies pretend to overcome part of these problems by using alternative materials, easy manufacturing techniques and non-expensive substrates. Between the absorbers proposed for these new thin film devices, $CuInSe_2$ (CIS) and its related quaternary alloy $Cu(Ga,In)Se_2$ (CIGS) have aroused interest because of their high absorption coefficient and their exceptional physical and chemical stability [3]. The use of these p-type semiconducting absorbers in combination with n-type CdS and ZnO transparent conductive oxide front contact has lead to record laboratory efficiencies of around 10-14% for CIS and 20% for CIGS [1].

There are multiple techniques currently available for the preparation of CIS thin films, for instance co-evaporation, RF sputtering, molecular beam epitaxy, metal organic chemical vapor deposition, spray pyrolysis, and electrodeposition [4]. Amongst them, electrodeposition is one of the most appealing because of the easiness of implementation, the comparatively reduced cost as it can be done at room temperature and the scalability at industrial level. Another interesting advantage of electrodeposition compared to evaporation or sputtering techniques is that deposition on substrates with non-planar form can be easily accomplished. Although several approaches for CIS electrodeposition have been described during the past decade [4,5,6], the majority of them are limited by the low crystallinity of the as-deposited layers [6] and the incorporation of Se and Cu-Se impurities that decrease the whole solar cell efficiency [5]. To improve the quality of these films, post-deposition treatments that require high temperatures in Se atmosphere and KCN etching have been reported [6,5]. Nevertheless, the direct electrodeposition of high crystallinity and good stoichiometry CIS films is still a challenge.

In this work, we propose a new CIS electrodeposition approach grounded on the successful phase control of $Cu_{2-x}Te$ films [7] and the pulsed electrodeposition of ZnO [8] developed in our group. The method [9] is based on the sequential application of short potential pulses at the electrodeposition potential of each element and the solid state

reaction when stepping back the potential to start the subsequent sequence of pulses, which is called cycle. The film microstructure is characterized by field emission scanning electron microscopy (FESEM) and Raman spectroscopy. The electrochemical photocurrent response demonstrates the photoactive behaviour of the obtained thin films. Additionally, films were characterized by X-ray diffraction (XRD), X-ray photoelectron spectroscopy (XPS) and near infrared (NIR) transmittance.

II. EXPERIMENTAL DETAILS

A. Sample and electrolyte

CIS layers were prepared onto indium tin oxide (ITO) coated glass substrates (Sigma Aldrich, 15-25 Ω/sq). Previous to film deposition, substrates were rinsed with ethanol and MilliQ water, N_2 blown and immediately mounted in the electrochemical cell. The electrodeposition bath was prepared by combining in the 1:1:1 ratio 10 mM $CuSO_4.5H_2O$, 10 mM $In_2(SO_4)_3.xH_2O$ and 10 mM SeO_2 solutions, from high purity reactants (Sigma Aldrich, up to 99.9+ pure). The resultant solution was conveniently diluted with MilliQ water (18 MΩ) to obtain final nominal concentrations of 2 mM and 0.3 mM with respect to Cu^{2+}, which will be called from herein high and low, correspondingly. The pH was adjusted with 0.1 M H_2SO_4 between 2.10 and 2.20 when working at high concentration and between 2.50 and 2.60 for low concentration. Before the experiments the electrolyte was bubbled with Ar (99.999%) to remove dissolved O_2.

B. Electrochemical measurements and film growth

Electrodeposition, cyclic voltammetry (CV) and photocurrent characterization were performed using a PGSTAT 12 Autolab potentiostat (Eco Chemie). A specially designed glass cell with the working electrode placed at the bottom, a large Pt/Ir wire as auxiliary electrode and a Ag/AgCl (SSC) reference electrode in contact with the solution through a Luggin capillary were employed. All the potentials from herein will be quoted versus the SSC electrode.

The behaviour of the electrochemical reactions during the deposition was studied before the film growth in order to determine the potential values that would be applied during the pulsed deposition. CVs of the electroactive species in separate solutions and of the background acid solution were acquired.

The film growth routine by the pulsed method consisted of repeated cycles of potential pulses of equal length, carefully placed at the electrodeposition potentials of Cu, Se and In respectively. Film thickness was controlled by the total number of cycles. From previous studies on the pulsed electrodeposition of ZnO we know that pulse duration has a strong effect in the microstructure [8] because it is directly related to the flux of each element approaching the electrode, especially when working in diluted electrolytes, therefore, films were prepared at different values of pulse duration: 0.5, 0.1 and 0.01 s for both high and low concentration electrolyte solutions. The number of cycles was recalculated to obtain comparable thicknesses. Alternatively, two samples were prepared in the high concentration electrolyte by sweeping the potential at 5 mVs^{-1} from the open circuit potential value to U_e=-500 and U_e=-600 mV and keeping it there for 1000 s.

C. Sample characterization

XRD measurements were done in a PANalytical X'Pert PRO MPD Alpha1 diffractometer using Cu K_α (λ=1.5418 Å) radiation in the Bragg-Brentano geometry. The phases were identified with the JCPDS database [10]. Surface morphology was characterized in a Hitachi H-4100 FESEM. NIR transmittance spectra were acquired in a Bomen DA3 spectrometer and the UV-Vis in a Specord 205 (Analytik Jena), in both cases using a clean ITO as reference. XPS was carried out in a PHI 5500 Multitechnique System (Physical Electronics) using a monochromatic Al K_α X-ray source (1486.6 eV energy and 350 W) perpendicular to the analyzer axis. The measurements were done in an ultra high vacuum (UHV) chamber between $5x10^{-9}$ and $5x10^{-8}$ Torr. The analyzed area was a 0.8 mm diameter circle and the resolution was 187.5 eV of pass energy and 0.8 eV/step for the general spectra while the mid resolution spectra of the different elements was 23.5eV of pass energy and 0.25 eV/step. In-depth composition was obtained by measuring after eroding the sample surface with Ar^+ ions from a 4 keV energy source. Composition was assessed from sample surface down to the glass substrate below ITO. Raman scattering analysis was performed in the backscattering configuration with the 514.5 nm line of an Ar^+ laser excitation source. Special care was taken to avoid sample damage by laser heating working at minimal power density.

The photocurrent measurements were performed in the electrochemical cell using a 0.1 M $NaNO_3$ electrolyte to avoid further reactions. The sample was irradiated with a 150 W illuminator (Dolan Jenner) from the solution side. Two different measurements were done: 1) the film was alternatively illuminated in 180 s on/off cycles at a steady potential while the photocurrent response was recorded; 2) A linear sweep voltammetry (LV) is recorded under illumination and in dark conditions.

III. RESULTS AND DISCUSSION

A. Electrochemical characterization and film growth

Fig. 1 shows the CV of the electrolytic bath used for film deposition that contains 2 mM Cu^{2+}, 2 mM Se^{4+} and 4 mM In^{3+} obtained using an ITO substrate as working electrode. For comparison, the CVs of the elements by separate and a CV of the 0.1 M H_2SO_4 supporting electrolyte are also included. It is noticeable that the supporting electrolyte causes an anodic current attributed to In dissolution from the ITO substrate after reaching potentials more negative than -1 V. Both substrate degradation and hydrogen evolution restrict the range of negative potentials that can be applied during the growth.

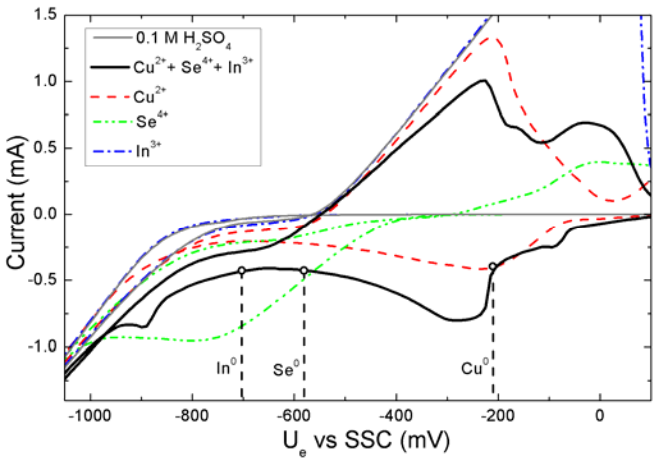

Fig. 1 *CV at 100 mVs^{-1} of the electrolytic bath containing 2mM Cu^{2+},2 mM Se^{4+} and 4mM In^{3+}used for CIS growth, those of the separate elements and the supporting electrolyte 0.1 M H_2SO_4 solution.*

With respect to single element CVs presented in Fig. 1, it can be mentioned that:

i) The reduction from Cu^{2+} to Cu^0 is accepted to occur by means of a global step via two electrons transference because the time for the existence of Cu^+ is very short and thus it is hardly detectable by CV techniques [11]. The process begins at around -210 mV and then proceeds by diffusion control. In the anodic sweep, a dissolution wave probably due to substrate damage is observed as well as Cu oxidation peaks attributable to Cu_2O formation at potentials greater than -100 mV.

ii) Se^{4+} is reduced in a complex mechanism involving dehydration of the aqueous selenium complex, formation of Se^0 and possibly Se^{2-} at potentials near hydrogen evolution [11]. Upon anodic sweep Se^0 prevents In dissolution from the ITO substrate.

iii) In reduction process on the ITO surface presents an overpotential evidenced by the delay of the anodic response. During the anodic sweep, at around -600 mV, strong dissolution of the previously deposited In takes place.

The elemental deposition reactions can be described by equations (1)-(3).

$$Cu^{2+} + 2e^- \rightarrow Cu^0 \qquad U_e = -210\ mV \qquad (1)$$

$$Se^{4+} + 4e^- \rightarrow Se^0 \qquad U_e = -580\ mV \qquad (2)$$

$$In^{3+} + 3e^- \rightarrow In^0 \qquad U_e = -700\ mV \qquad (3)$$

The In and Se deposition potentials in the mixture containing all the species tend to appear at less negative values than those in the single component solutions. This phenomenon is known as Kroger's mechanism [12]. The electrode potentials indicated in Fig.1 U_e=-210, U_e=-580 and U_e=-700 mV were chosen to keep the elements deposition for CIS growth out of diffusion regime.

Fig. 2a displays the current response to the potential application routine used to grow the samples by pulsed electrodeposition. The applied potential is kept for 0.5 s at the electrodeposition potentials discussed above, and then is stepped back to the initial Cu electrodeposition potential to start the subsequent cycles. The current response at each potential shows an initial nucleation peak that afterwards reaches a limit value. During the first cycle the current response at -210 mV is dominated by the Cu electrodeposition, then at -580 mV elemental selenium and also $Cu_{2-x}Se$ phases are formed according to equations (2) and (4), respectively. In the last step, at -700 mV, the In inclusion reaction within the Cu-Se binary phases to form the final CIS compound as shown in (5) and the elemental deposition of In like in (3) coexist [13].

$$Cu^0 + Se^{4+} \rightarrow Cu_{2-x}Se \qquad (4)$$

$$Cu_xSe_y + In^{3+} \rightarrow CuInSe_2 \qquad (5)$$

After the first cycle, the return to more positive potentials to start the subsequent three steps dissolves the excess of metallic

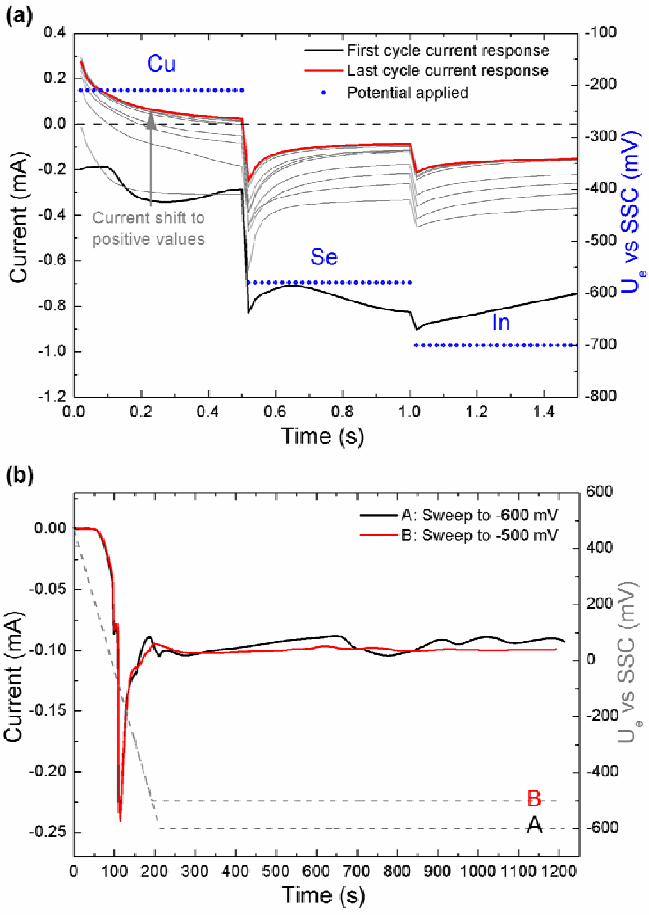

Fig. 2 (a) *Potential application routine and current response evolution along cycles obtained for a pulsed electrodeposition growth with 0.5 s pulse duration in the high concentration solution. The total deposition time is 20 minutes.* ***(b)*** *Potential applied and current response for samples grown by potential sweep (5mVs^{-1}) to U_e=-500 and U_e=-600 mV combined with fixed potential in the high concentration electrolyte solution.*

In and enhances the formation of the desired CIS phase by polarizing positively the deposited species. This polarization is likely to force the oxidation of metallic Cu to Cu^+ inside the deposited mixture with no contribution to the current response, a similar approach to the solid state reaction referred for $Cu_{2-x}Te$ films [7]. The reaction of In dissolution is evidenced experimentally by a shift in the current towards positive (anodic) values at -210 mV as the number of cycles increases.

Conversely, Fig.2b shows the current response for samples grown by potential sweep from open circuit potential to U_e=-500 and U_e=-600 mV to assess the compositional and microstructural changes. At -80 mV a small nucleation peak that would correspond to the Cu underpotential deposition is observed before the main reduction peak at around -130 mV. The potential shift with respect to that in Fig. 1 is explained because of the lower sweep rate. After the Cu nucleation step, Se deposition begins at around -300 mV and thereafter current oscillations are observed during the whole film growth.

B. *Structure and morphology*

The as-grown films are adherent and dark-brown coloured. Fig.3 shows the normalized X-ray diffractograms of the films described in the experimental section, all of them exhibiting the chalcopyrite $CuInSe_2$ phase oriented in the (112) direction. This orientation is believed to be the most advantageous for lattice matching with n-CdS [11]. The considerable peak width indicates the nanocrystalline quality of the films. The patterns A and B which correspond to the samples prepared by potential sweep combined with fixed potential at U_e=-600 and U_e=-500 mV respectively, reveal a shoulder at lower Bragg angle that can be associated to the presence of binary Cu_2Se. This phase is not detected for the other electrodeposited films (C-H) grown by the pulsed method. Although crystallinity is still low, further improvements are devised either by in-situ thermal or electrochemical treatments.

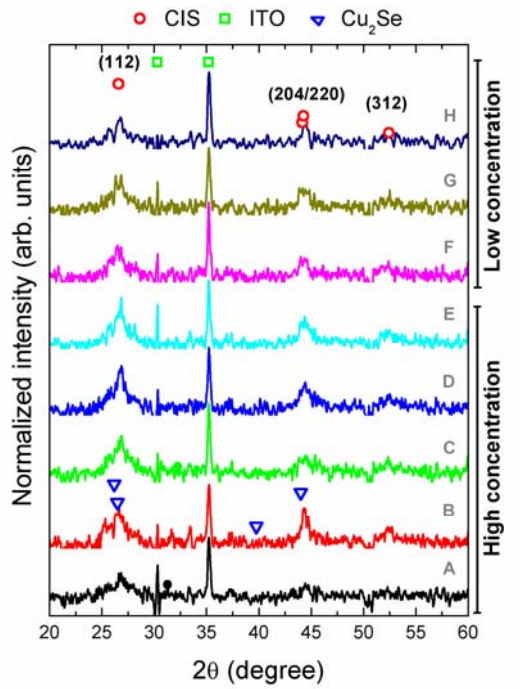

***Fig.3**. XRD of the films prepared with the high electrolyte concentration at fixed electrode potentials (A) U_e=-600 mV and (B) U_e=-500 mV, and also with the pulsed electrodeposition at pulse durations of (C) 0.5, (D) 0.1, and (E) 0.01 s. (F-H) Correspond to samples prepared at low concentration and at the same pulse durations as in (C-E). PDF cards: 401487 (CIS), 391058 (ITO) and 371187 (Cu_2Se).*

Morphology makes an evident evolution from those samples prepared by potential sweep and fixed electrode potentials (Fig.4 A-B) to the ones prepared with the pulsed programmed routine at the same concentration (Fig.4 C-E). In the first case, we observe agglomerates spread all over the sample and uneven grain sizes that make the sample poor in uniformity and very rough. The films obtained using the pulsed electrodeposition routine have a more homogeneous morphology in terms of grain size and height of the features, which is noticeably improved by shortening the pulse duration and decreasing the electrolyte concentration (Fig.4 F-H).

C. *Optical characterization*

NIR and UV-Vis transmittance spectra have been acquired in samples prepared at half deposition time to enhance the transmitted light signal. The cut in the spectra shown in Fig. 5a is due to detector limits in the used equipment. In the UV-Vis wavelength range (300-700 nm) of the transmittance spectra presented in Fig. 5a, an absorption associated to Cu-Se phases is observed [14]. On the other hand, in the NIR range (900-2150 nm) the CIS phase has the main effect on the optical absorption. The small shift on the maxima of the oscillations in the spectra indicates that thicknesses are kept almost constant; hence, the changes in transmittance are produced by variations in the absorption coefficient.

As two phases determine the optical behaviour of the films, two optical band gaps were calculated on the basis of the optical absorption spectra, using the well-known Tauc relation in (6):

$$\alpha h\nu = A(h\nu - E_g)^n \qquad (6)$$

where A is a constant, hν is the photon energy, α is the absorption coefficient, and n depends on the nature of the transition but for direct transitions n = ½ [14]. The plot is presented as the variation of $(\alpha h\nu)^2$ vs hν, in which the E_g energy can be found by extrapolating the linear portion of the plot to the energy axis at α=0 [11] as shown in Fig.5b and 5c.

In the Tauc plot of the NIR range, Fig. 5b, the films E_g values are in the range of 1.1-1.25 eV which correspond to the CIS phase. At energies lower than the E_g, an absorption feature is evident. This band can be related to impurity states [11] or to the ordered vacancy compound (OVC) that has been frequently reported in electrodeposited CIS films [15]. In Fig. 5c, the calculated E_g values range from 2.7 to 3.1 eV. Although great dispersion of the reported E_g values for different Cu-Se phases, both Cu(I), Cu(II) and mixed valence compounds was found in the literature [14,16,17], we assume $Cu_{2-x}Se$ presence considering the evidence from XRD. This will be further discussed in sections below.

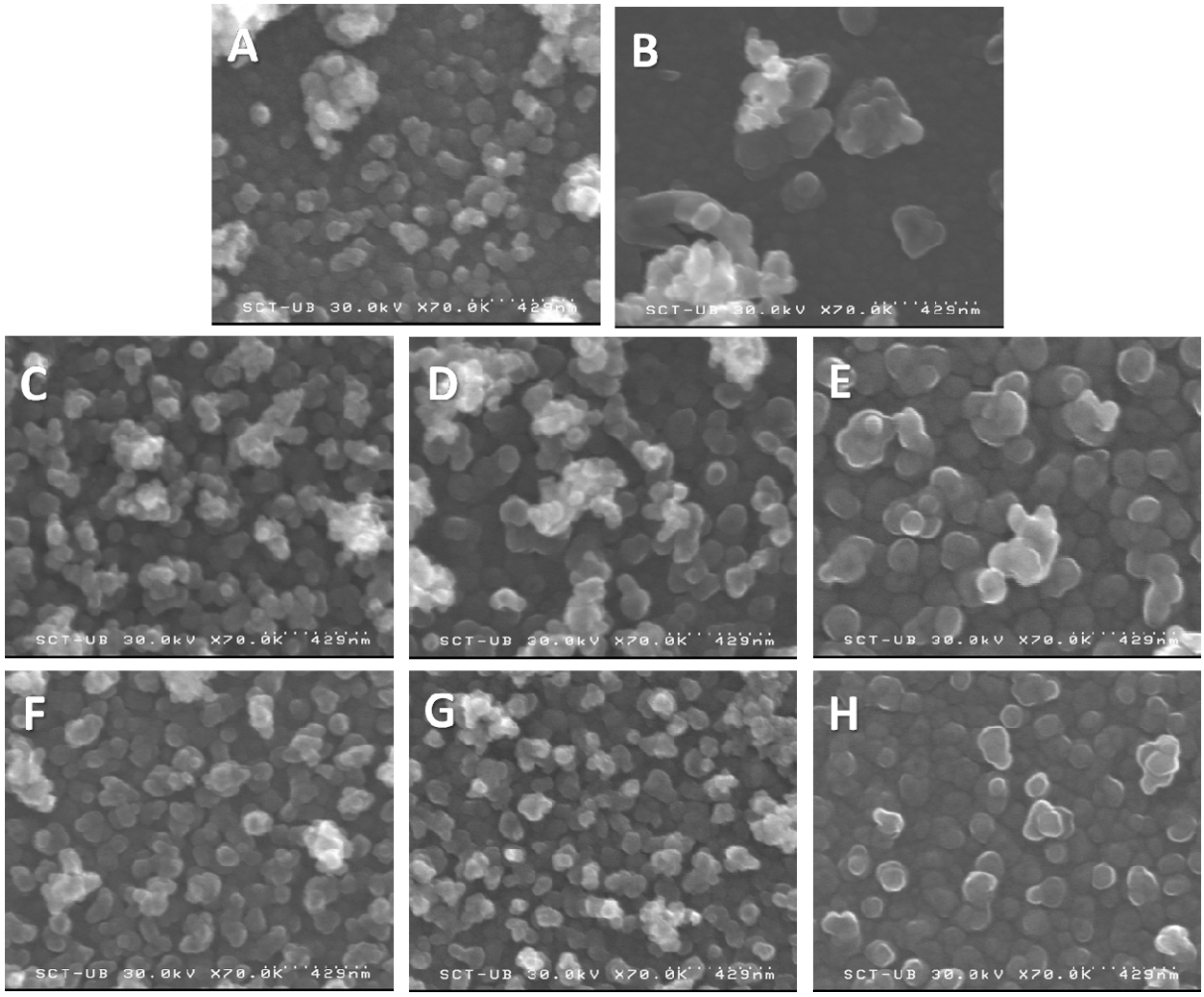

Fig. 4 *FESEM images of the films prepared with the high concentration at (A) U_e= -600 mV, (B) U_e= -500 mV, and with the pulsed potential program at different pulse durations of (C) 0.5, (D) 0.1 and (E) 0.01 s. Samples from F to C correspond to samples prepared at low concentration using the same pulse durations described in (C-E).*

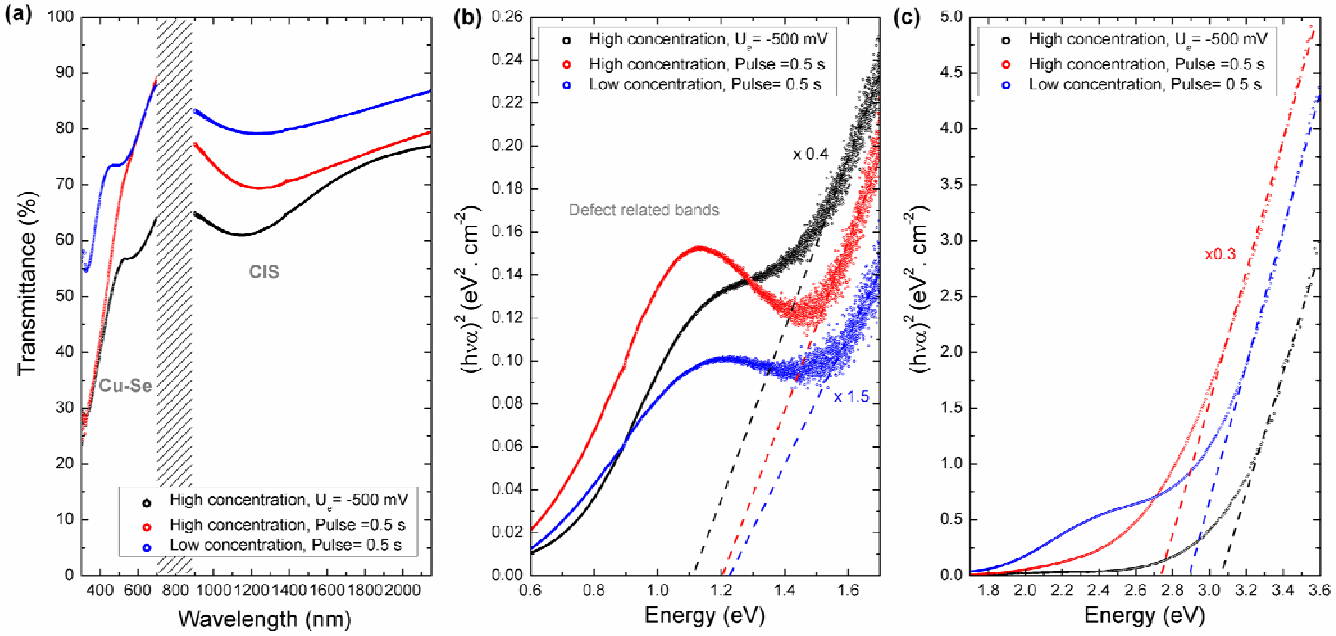

Fig. 5(a)*Transmittance spectra of samples prepared at U_e= -500 mV in the high concentration electrolyte and with the pulsed potential program with 0.5 s pulse duration at both high and low concentration* ***(b)*** *and* ***(c)*** *plot of $(h\nu\alpha)^2$ vs hν in the NIR and UV-Vis ranges, respectively, of the same samples.*

D. Chemical and microstructural characterization

A representative XPS survey spectrum of the samples is shown in Fig. 6a. The spectrum indicates the presence of Cu, In and Se but also a large O 1s core-level signal due to surface oxidation, which has been described as a common issue for CIS films [18].

In Fig. 6b a series of in-depth mid-resolution XPS spectra in the region of Se 3d, In 3d5 and Cu 2p core levels is presented. These spectra correspond to the whole film thickness just before arriving to the ITO substrate. It can be appreciated that the peak shape and position remains constant through the CIS film, denoting the same chemical environment and oxidation state. The presence of neither Cu^{2+} nor different Se species is manifested at the resolution employed in these measurements [13]. The atomic composition along the profile is not presented since to obtain reliable data we should avoid or at least know the etch-induced alteration of the composition. The standard method of Ar^+ ion sputtering has been found to produce significant surface damage such as In enrichment or Cu depletion in CIS [18]. In our samples we have appreciated this In enrichment, thus we consider that the calculated composition is not representative.

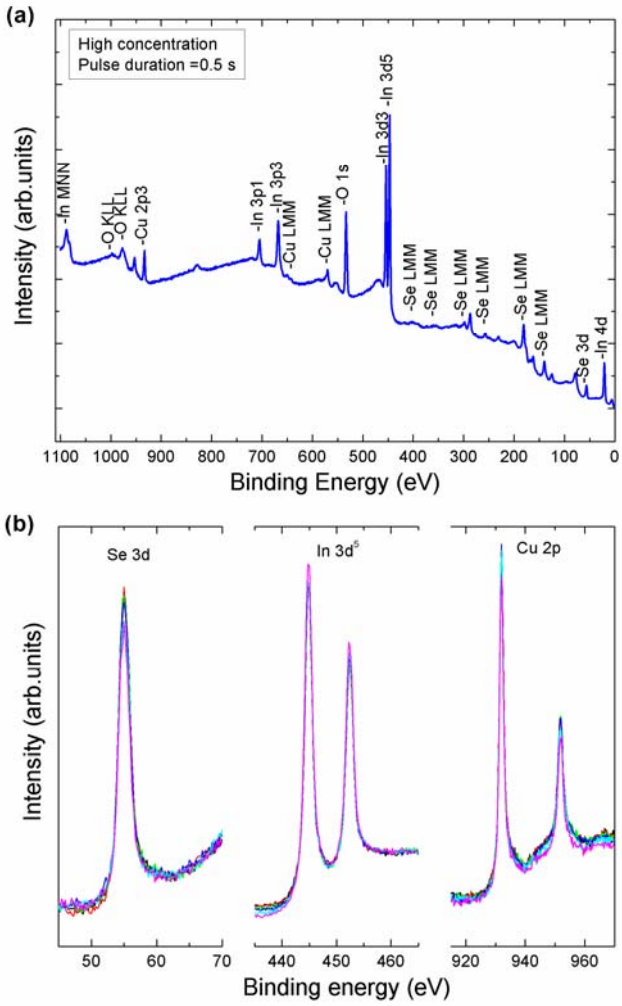

Fig.6 (a) *XPS survey spectra of a CIS film obtained by pulsed electrodeposition using the high concentration bath and 0.5 s pulses.* ***(b)*** *Mid-resolution Se 3d, In 3d5 and Cu 2p core level spectra of the same sample.*

Raman spectroscopy is a very powerful tool to study composition and structure evolution in poorly crystalline or amorphous materials [19]. Particularly, Raman spectroscopy has been widely used to characterize the phase composition in electrodeposited CIS films [13,15,20]. Fig. 7 shows the background-subtracted Raman spectra in the 140-280 cm^{-1} range and the analysis of the identified bands. The insets depict the spectra deconvolution using Lorentzian functions [19] into the following bands: the Ordered Vacancy Compound (OVC) at 160 cm^{-1} [15,20] which is formed as a result of copper deficiency during crystal growth and is characterized by the formation of an ordered array of point defects in the primary structure [20]; the A1 mode of CIS at 178 cm^{-1} [13,15,20]; the CIS overtones 2E, B1 and B2 grouped under a broad band at 215 cm^{-1} and whose presence is indicative of increased ordering [20]; the elemental Se associated band at 240 cm^{-1} [13,15,20]; and finally the Cu-Se compounds related band at 260 cm^{-1} [13,15,20]. Although it is not shown in Fig.7a, other Cu-Se bands hindered by a strong baseline were also observed in the samples prepared by potential sweep combined with constant potential in the spectrum range from 30 to 60 cm^{-1}[20]. These Cu-Se bands were particularly strong for the CIS films prepared at U_e= -600 mV in correspondence to the high Cu-Se band observed at 260 cm^{-1}. Other bands detected in Fig.7a are the ones related to OVC and elemental Se. The films prepared by pulsed electrodeposition using the same concentration as in the sweep, Fig.7b, also present the bands associated to Cu-Se, OVC and Se but their content does not seem to be significantly affected by the pulse duration. In contrast, in the films obtained by the pulsed method with the low concentration electrolyte (Fig. 7c) the Cu-Se band is absent and the pulse duration seems to have influence in the Se band intensity.

To compare the band intensities of all the samples, the integral ratios of each band obtained from the spectra deconvolution were normalized with respect to the A1 mode of CIS. These relative intensities can be correlated to the relative content of each phase in the sample [19,20]. In Fig. 8 the relative phase contents are presented as function of growth method and the electrolyte concentration. It can be seen that the samples prepared by potential sweep combined with a constant potential, present the highest relative contents of OVC, Se and Cu-Se. Cu-Se phases are known to be a prerequisite to In incorporation [13], however, as discussed before, the slow sweep growth makes the formation of Cu-Se concurrent with the In incorporation. If the In uptake is not enough to form the stoichiometric compound, then these Cu-Se would remain in the matrix. The OVC content indicates that also phases with low Cu content coexist. At the same concentration but with the pulsed potential program the final composition recalls to the one of the film obtained at U_e=-500 mV, therefore in this case the pulsed method does not improve the phase ratio, even though it enhances the uniformity of the film morphology.

On the other side, the samples prepared in the low concentration electrolyte by the pulsed method show no Cu-Se

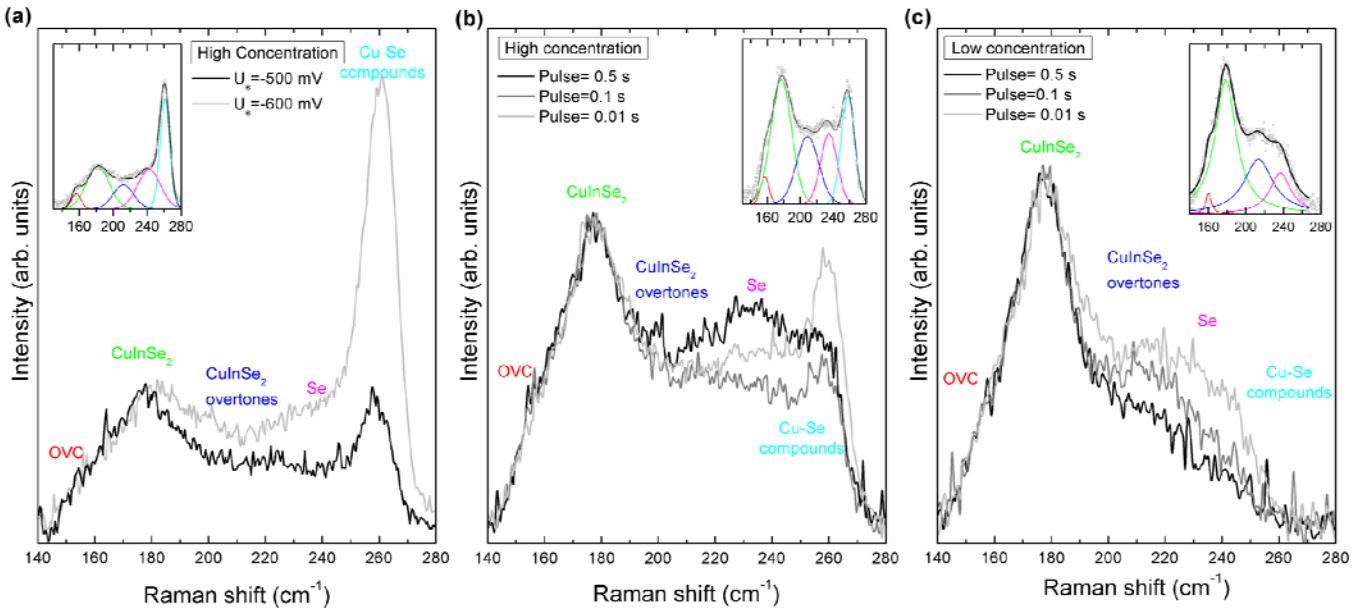

Fig. 7 *Background-subtracted Raman spectra in the region between 140 and 280 cm^{-1} of* ***(a)*** *CIS films prepared by potential sweep combined with constant potential at U_e= -600 and U_e=-500 mV* ***(b)*** *Films obtained by pulsed electrodeposition in the high concentration electrolyte using three different pulse durations 0.5, 0.1 and 0.01 s* ***(c)*** *Films prepared by pulsed electrodeposition in the low concentration electrolyte using the same pulse durations as in (b).*

related compounds and a decrease of one order of magnitude in the Se content and OVC with respect to the rest of the samples. It is possible to say that the film microstructure is enhanced at this electrolyte concentration by increasing pulse duration. This improvement can be attributed to the more controlled supply of material arriving to the electrode surface given by the pulsed application of potentials out of the diffusion regime, effect which is more perceptible at low concentrations.

E. Optoelectronic characterization

Fig. 9 shows the photocurrent response under intermittent illumination of a CIS film at increasing cathodic potentials while the inset displays the linear sweep voltammetry of the same film under illumination and dark conditions. Upon application of negative potentials electrons from the conduction band are extracted, so for a p-type semiconductor it is well-known that the current response (cathodic current) will be limited to a low level since the electron density in the conduction band is extremely small [21]. However, if we illuminate with light of higher energy than the E_g, electrons are promoted from the valence band to the conduction band, enhancing the cathodic current response [21]. This effect can be clearly appreciated in the inset of Fig. 9 where the cathodic current is higher under light conditions, thus confirming the p-type character of the deposited CIS films.

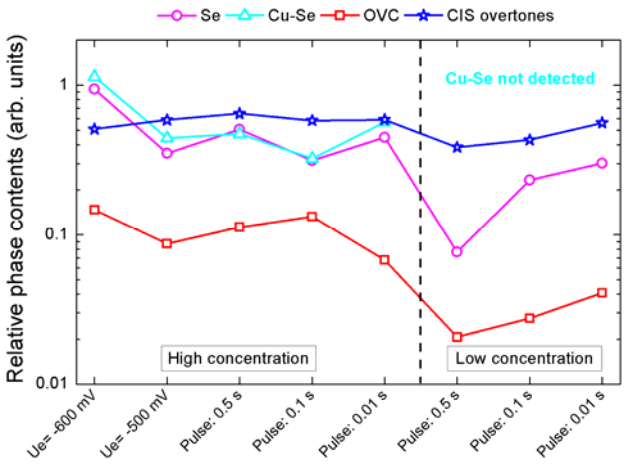

Fig.8 *Relative phase content obtained by normalization of the deconvoluted Raman band intensities with respect to the A1 CIS mode. The results are presented as function of the sample growth conditions.*

From the intermittent light measurement in Fig. 9, it can be observed that at increasing negative potentials the current response is higher as expected at potentials below photocorrosion [21]. Also qualitative information about the photogeneration of the minority charge carriers and recombination processes can be extracted from this measurement. During the illumination period, the photogeneration of electrons appears to be formed by two different processes: an initial fast step denoted by a strong increase of the cathodic photocurrent which corresponds to valence band to conduction band excitations inside the CIS film; a second step that proceeds slowly, and that can be attributed to the transference of excited electrons from the impurity levels to the conduction band of the CIS matrix or even from the secondary Se or Cu-Se phases. When the light is off it can be appreciated that photocurrent is not interrupted steeply but it decreases slowly until reaching the original dark current level. This suggests a relatively high lifetime of the photogenerated charge carriers that could be ascribed to slow electron release from trap levels. Further studies with time resolved photocurrent spectroscopy or wavelength dependent

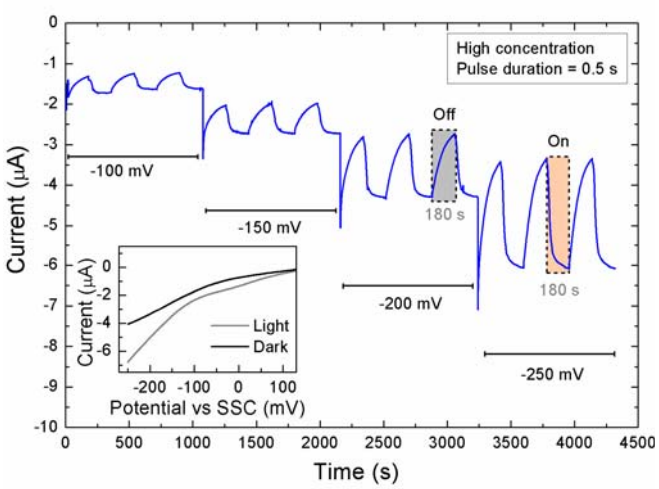

Fig.9 *Photocurrent response at different potentials of the sample prepared at high electrolyte concentration and 0.5 s pulse duration. Intermittent illumination cycles of 180 s amplitude were used. The inset shows the linear sweep voltammetry at 1mVs^{-1} under dark and illumination conditions.*

charge carrier excitation will be of great use to understand better all the described processes.

In order to compare the photocurrent response between the CIS films obtained in different growth conditions, the photocurrent amplitude was calculated from the respective measurements at an applied potential of -200 mV. The obtained values are presented in Table 1. It can be seen that the samples obtained by potential sweep until U_e=-500 mV present the lower photocurrent response. Considering that in the Raman analysis the relative phase contents of the above-mentioned sample were similar to the one prepared by 0.5 s pulses in the high concentration electrolyte, therefore this effect cannot be related to the phase impurities but to the increased scattering caused by the less uniform morphology of the former one. The higher light scattering in that sample is evidenced by the lower transmittance already shown. The best photocurrent response is achieved by the sample prepared by the pulsed electrodeposition program in the low electrolyte concentration. The origin of this enhancement can be the synergic effect between a more uniform morphology and a lower content of Se or Cu-Se phases.

TABLE I
PHOTOCURRENT RESPONSE

Growth conditions	Photocurrent amplitude at -200 mV
High concentration, Sweep U_e= -500 mV	-0.34 μA
High concentration, Pulse duration= 0.5 s	-1.61 μA
Low concentration, Pulse duration= 0.5 s	-3.73 μA

IV. CONCLUSIONS

A new method for electrodeposition of $CuInSe_2$ thin films has been developed. It consists in the application of cycles formed by three potential pulses that correspond to Cu electrodeposition, elemental Se and Cu-Se formation and In reduction together with further incorporation in the previously formed Cu-Se. By the careful election of these potentials, the formation of CIS occurs out of the diffusion regime. For the sake of comparison samples prepared by potential sweep combined with a constant potential step were also grown. The new developed pulsed method allows the attainment of nanocrystalline films oriented in the (112) direction with a more uniform morphology than those acquired by the sweep/step routine. From the optical measurements, we inferred that samples presented two optical band gaps (E_g), one of them corresponding to the CIS matrix at around 1.1 eV, and another between 2.7 and 3.1 attributed to Cu-Se phases. The XPS results reveal that the film surface is partially oxidized by contact with atmospheric oxygen, but after the removal of this layer in-depth chemical environment of the species remains constant. Atomic quantification was not possible from XPS measurements due to the In enrichment caused by the Ar^+ sputtering. To assess the presence of other phases apart from CIS, Raman spectroscopy analysis was performed. It was found that Cu-Se was present in samples grown by potential sweep/step and by pulsed electrodeposition in the high concentration electrolyte. On the contrary, when working with the pulsed method in the low concentration electrolyte the Raman band related to Cu-Se compounds was not present. Also an influence of pulse duration on the Se content was notorious, achieving lower contents at longer pulse durations. Finally, the photocurrent response of the films was characterized to confirm the p-type character of the films. Under intermittent light conditions two processes of carrier photogeneration seem to occur: a fast one from CIS band-to-band transitions and a slower one that could be related with impurity levels. The non-abrupt decrease in the photocurrent when light is turned off suggests a relatively high lifetime of the generated photoelectrons. The photocurrent response is clearly higher for samples prepared by pulsed electrodeposition. Amongst them, working at low electrolyte concentrations the best performance is achieved. This fact is related to the cooperative effect of the film uniformity and the lower content of impurity phases.

APPENDIX

Parts of this work have been exposed at the European Energy Conference held in Barcelona between April 20th -23rd 2010 and will be presented in the 8th International Symposium on Electrochemical Micro and Nanosystem Technologies that will take place in Cannes-Mandelieu between September 21st-23rd 2010.

ACKNOWLEDGMENT

Author thanks Dr. Octavio Calzadilla (invited Professor from Universidad de La Havana) for the valuable discussion on the optical measurements. The Scientific Technical Services at University of Barcelona (SCT-UB), particularly the XRD, SEM, XPS and Molecular Spectroscopy Units are also acknowledged. Financial support from IBEC and MEC

through the CTQ2007-68101-C02-01 project is recognized.

REFERENCES

[1] A. Slaoui, R.T. Collins, "Advanced Inorganic Materials for Photovoltaics", *MRS Bull*.,vol. 32, pp. 211-218, March 2007.

[2] A. D. Compaan, "Photovoltaics: Clean power for the 21st century", *Sol. Energy Mater. Sol. Cells*, 90, pp. 2170-2180, 2006.

[3] J.F. Guillemoles, "The puzzle of $Cu(In,Ga)Se_2$ (CIGS) solar cells stability", *Thin Solid Films*, 403-403, pp. 405-409, 2002.

[4] F.Kang, J. Ao, G. Sun, Q. He, Y. Sun, "Structure and photovoltaic characteristics of $CuInSe_2$ thin films prepared by pulse-reverse electrodeposition and selenization process", *J. Alloy Comp.,* 478, pp. L25-L27, 2009.

[5] E.Saucedo *et al*., "Key role of Cu-Se binary phases in electrodeposited $CuInSe_2$ precursors on final distribution of Cu-S phases in $CuIn(S,Se)_2$ absorbers", *Thin Solid Films,* 517, pp. 2268-2271, Nov. 2008.

[6] J.S. Wellings, A.P. Samantilleke, S.N. Heavens, O. Warren, I.M. Dharmadasa, "Electrodeposition of $CuInSe_2$ from ethylene glycol at 150ºC", *Sol. Energy Mater. Sol. Cells*, 93, pp. 1518-1523, May 2009.

[7] F. Caballero-Briones, A. Palacios-Padrós, F.Sanz, "Phase tailored, potentiodynamically grown p-$Cu_{2-x}Te$/Cu layers", *Electrochem. Comm*., 10, pp. 1684-1687, Aug. 2008.

[8] F. Caballero-Briones, A. Palacios-Padrós, O. Calzadilla, F. Sanz, "Pulsed electrodeposition of ZnO films", unpublished.

[9] A. Palacios-Padrós, F. Caballero-Briones, F. Sanz, "Enhancement in as-grown $CuInSe_2$ film microstructure by a three potential pulsed electrodeposition method", *Electrochem. Comm*., 12, pp.1025-1029, Aug. 2010.

[10] International Centre for Diffraction Data, "Powder Diffraction Files-2 Database", PA, USA, 2000.

[11] T.P. Gujar *et al.*, "Characterization of electrochemically grown crystalline $CuInSe_2$ thin films", *J. Electrochem. Soc*., 156, pp. E8-E12, Nov. 2009.

[12] D. Lincot *et al*., "Chalcopyrite thin film solar cells by electrodeposition", *Sol. Energy*, 77, pp. 725-737, May 2004.

[13] O.Roussel *et al.*, "First stages of $CuInSe_2$ electrodeposition from Cu(II)-In(III)-Se(IV) acidic solutions on Polycrystalline Mo films", *J. Electrochem. Soc.,* 155, pp. D141-147, Dec. 2007.

[14] B. Pejova, I. Grozdanov, "Chemical deposition and characterization of Cu_3Se_2 and CuSe thin films", *J. Solid State Chem.*, 158, pp. 49-54, March 2001.

[15] X. Fontané, "In-depth resolved Raman scattering analysis of secondary phases in Cu-poor $CuInSe_2$ based thin films", *Appl. Phys. Lett*., 95, pp.121907, 2009.

[16] R. Vaidyanathan, M. K. Mathe, P. Sprinkle, S. M Cox, U. Happek, J. L. Stickney, "Electrodeposition of Cu_2Se Thin Films by Electrochemical Atomic Layer Epitaxy (EC-ALE)", in *MRS Proceedings*, Warrendale, PA, USA, 744, pp.M5.34, 2002.

[17] R. H. Bari, V. Ganesan, S. Potadar, L. A. Patil, "Structural, optical and electrical properties of chemically deposited copper selenide films", *Bull. Mater. Sci.*, 1, pp.37-42, Feb. 2009.

[18] K. Otte, G. Lippold, D. Hirsch, A. Schindler, F. Bigl, "XPS and Raman investigations of nitrogen ion etching for depth profiling of $CuInSe_2$ and $CuGaSe_2$", *Thin Solid Films*, 361-362, pp.498-503, 2000.

[19] F. Caballero-Briones et al., "Structural analysis of Cd-Te-O films prepared by RF-reactive sputtering", *J. Non-Cryst. Sols.*, 354, pp. 3756-3761, May 2008.

[20] V. Izquierdo-Roca *et al.*, "Raman scattering characteristics of electrochemical growth of $CuInSe_2$ nanocrystalline thin films for photovoltaic applications: Surface and in-depth analysis", *Surf. Interface Anal.*, 40, pp. 798-801, Jan. 2008.

[21] R. Memming, "Semiconductor Electrochemistry", Weinheim:Wiley-VCH, 2001, 167-178.